





Communication

# Sulphate Removal in Industrial Effluents Using Electrocoagulation Sludge as an Adsorbent

Siyanda Yamba<sup>1,2</sup>, Nomso C. Hintsho-Mbita<sup>3</sup> , Tunde L. Yusuf<sup>1</sup> , Richard Moutloali<sup>1,4</sup>   
and Nonhlangabezo Mabuba<sup>1,\*</sup> 

<sup>1</sup> Department of Chemical Sciences, University of Johannesburg, P.O. Box 170111, Doornfontein 2028, South Africa

<sup>2</sup> Buffalo City Metro Municipality, Scientific Services, No. 1 Reservoir Road, Selbone, East London 5201, South Africa

<sup>3</sup> Department of Chemistry, University of Limpopo, Sovenga, Polokwane 0727, South Africa

<sup>4</sup> Department of Science and Technology, Mintek-Nanotechnology Innovation Centre, University of Johannesburg, Johannesburg 2006, South Africa

\* Correspondence: nmabuba@uj.ac.za

**Abstract:** The high concentration of sulphates is detrimental to the infrastructure of wastewater treatment plants. Hence in this study, we present the application of electrocoagulation sludge as an adsorbent to remove sulphates from industrial effluents before they are released back to the environment. The sludge contains iron and aluminium cations and cationic complexes that precipitate sulphates in water. Corrugated iron sheet was used as a sacrificial electrode during electrocoagulation (EC) to generate sludge. FTIR, XRD, SEM, TEM, and Zeta Potential were used to characterize the sludge. The following parameters: contact time, pH, initial concentration, and adsorbent dosage were optimized to 120 min, 2, 100 mg/L and 150 mg, respectively. For the synthetic water, the sulphate removal was 99.1%, whereas for the real water it was found to be 98.7%. The adsorption capacity of the EC sludge was 66.76% for 2 h under acidic conditions. The Langmuir isotherm fitted better than the Freundlich isotherm. This confirmed the homogenous distribution of the active sites on the EC sludge. At different EC's sludge, the pseudo-second order kinetic model produced the best fitting experimental results which confirmed the removal of sulphate ions by chemisorption. This approach (method) is useful for purifying industrial effluents before they are discharged into the environment.

**Keywords:** electrocoagulation sludge; recycling; wastewater treatment; sulphates; adsorbent



**Citation:** Yamba, S.; Hintsho-Mbita, N.C.; Yusuf, T.L.; Moutloali, R.; Mabuba, N. Sulphate Removal in Industrial Effluents Using Electrocoagulation Sludge as an Adsorbent. *Sustainability* **2022**, *14*, 12467. <https://doi.org/10.3390/su141912467>

Academic Editor: Paolo S. Calabrò

Received: 15 August 2022

Accepted: 27 September 2022

Published: 30 September 2022

**Publisher's Note:** MDPI stays neutral with regard to jurisdictional claims in published maps and institutional affiliations.



**Copyright:** © 2022 by the authors. Licensee MDPI, Basel, Switzerland. This article is an open access article distributed under the terms and conditions of the Creative Commons Attribution (CC BY) license (<https://creativecommons.org/licenses/by/4.0/>).

## 1. Introduction

Recycling and reusing industrial and organic waste is crucial to preserve our ecosystem [1]. This approach aids in resolving environmental issues such as the volume of waste sent to landfills and incinerators, and creates opportunities for economic gains through the preservation of natural resources such as timber, water, and minerals, as well as improvement in economic security using domestic resources [2,3]. The salvage of improved commodities from the waste is undoubtedly one of the most crucial phases of waste management [4].

Due to the severe lack of affordable housing in developing countries, many low-income and poor households were forced to live in the country's expanding shanty towns, that the country's National Housing Code characterized as having/being: unsuitable places, unlawfulness and casualness, destitution and susceptibility, social stress, and environmental pollution [5]. Low-income and impoverished households constructed from low-cost substances such as outdated corrugated iron sheet, cupboards, plastics, and planks lead to authorized landfill sites and the problem of waste management [4]. The majority of the scrap old corrugated iron sheets are usually disposed of into the landfills; the hazards connected with this material might result in environmental concerns such as soil and

ground water contamination [4]. Corrugated iron sheet disposal through landfills is both uneconomical and unsustainable. As a result, a workable approach is to recycle it in order to generate sludge, which can then be utilized as a raw material in a variety of wastewater purification processes.

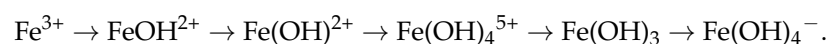
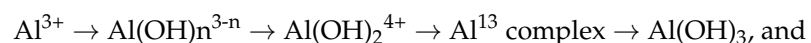
Recently, several wastewater treatment plants in the Buffalo City Municipality, Eastern Cape, South Africa were severely impacted by the untreated industrial effluents containing high concentrations of sulphate. The high concentration of sulphates destroys sewer lines, and forms acids that react with the water treatment pipelines [6]. In the reaction process, the hydrogen sulphide (H<sub>2</sub>S) that is produced corrodes both the pipelines and the storage tanks used for reticulation and treatment processes, thus, resulting in secondary contamination and deterioration of the infrastructure as well as the reduction of the life span of wastewater treatment plants that make the cement wall to crack as a result of the production of large amounts of sulphate ion [6].

There are a variety of conventional techniques that have been used successfully to remove sulphate ions, including ion exchange, biological treatment, chemical precipitation, and adsorption technologies. However, several of these techniques have disadvantages of their own [7]. When treating precipitation, enormous amounts of sludge are produced, and ion exchange and biological treatment usage is expensive. Adsorption, equally, is preferred because of how quickly and effectively it can remove anions. The most popular adsorbents are BaCl<sub>2</sub>, CaCl<sub>2</sub>, and ZrO(OH)<sub>2</sub>. However, BaCl<sub>2</sub> and ZrO(OH)<sub>2</sub> are costly, and BaCl<sub>2</sub> pollutes the environment [8]. In addition, the expected outcome of CaCl<sub>2</sub> wastewater filtration has not been achieved. Therefore, it is crucial to develop a sulphate adsorbent that is both effective and inexpensive and can possibly eliminate sulphate ions from wastewater [9].

Electrocoagulation (EC) has been shown as an effective approach for the elimination of sulphates by generating precipitants/adsorbents/coagulants from iron, zinc, or aluminium using a sacrificial electrode [10]. The removal methods in electrocoagulation (EC) are affected by water composition, pH, and Redox—potential, as shown in the aluminium and iron solubility diagram in Figure 1 [10]. During the oxidation of the sacrificial anode, aluminium forms polymeric species, such as

[Al<sub>6</sub>(OH)<sub>15</sub>]<sup>3+</sup>, [Al<sub>7</sub>(OH)<sub>17</sub>]<sup>4+</sup>, [Al<sub>8</sub>(OH)<sub>20</sub>]<sup>4+</sup>, [Al<sub>13</sub>O<sub>4</sub>(OH)<sub>24</sub>]<sup>7+</sup>, and [Al<sub>13</sub>(OH)<sub>34</sub>]<sup>5+</sup>, are formed and eventually transformed into Al(OH)<sub>3</sub>(s), which acts as a coagulate or flocs during the adsorption of sulphate ion. Similarly, Ferric ions produced by electrochemical oxidation of iron electrodes can create monomeric species, such as Fe(OH)<sub>3</sub>, as well as polymeric hydroxy complexes, Fe(H<sub>2</sub>O)<sub>6</sub><sup>3+</sup>, Fe(H<sub>2</sub>O)<sub>5</sub>(OH)<sup>2+</sup>, Fe(H<sub>2</sub>O)<sub>4</sub>(OH)<sup>2+</sup>, Fe<sub>2</sub>(H<sub>2</sub>O)<sub>8</sub>(OH)<sub>2</sub><sup>4+</sup> and Fe<sub>2</sub>(H<sub>2</sub>O)<sub>6</sub>(OH)<sub>4</sub><sup>4+</sup> [11].

The flocs of Al(OH)<sub>3</sub>(s) are isolated from the solution by sedimentation or flotation due to their substantial surface area for efficient adsorption. Ferric ions produced by electrochemical oxidation of iron electrodes can create monomeric species, such as Fe(OH)<sub>3</sub>, as well as polymeric hydroxy complexes, Fe(H<sub>2</sub>O)<sub>6</sub><sup>3+</sup>, Fe(H<sub>2</sub>O)<sub>5</sub>(OH)<sup>2+</sup>, Fe(H<sub>2</sub>O)<sub>4</sub>(OH)<sup>2+</sup>, Fe<sub>2</sub>(H<sub>2</sub>O)<sub>8</sub>(OH)<sub>2</sub><sup>4+</sup> and Fe<sub>2</sub>(H<sub>2</sub>O)<sub>6</sub>(OH)<sub>4</sub><sup>4+</sup> [12]. Furthermore, these species are gelatinous in origin and serve as precursors to the development of stable insoluble Al(OH)<sub>3</sub> flocs, which then remove contaminants via co-precipitation [13,14]. This is illustrated by the dependence of aluminium and iron polynuclear hydroxo complexes formation.



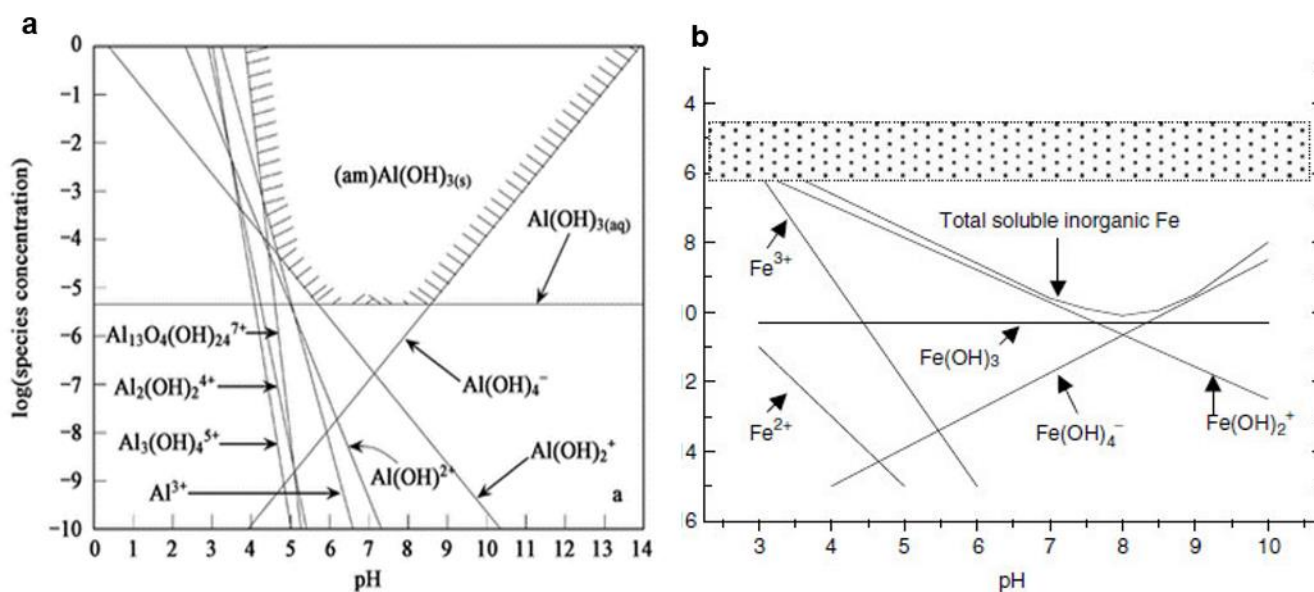


**Figure 1.** The diagram of theoretical (a) aluminium and (b) iron solubility in equilibrium with amorphous  $Al(OH)_3$  [14,15].

Both Al and Fe occurs in acidic and basic range as illustrated in the solubility diagrams (Figure 1a,b).

The equilibrium isotherms, thermodynamic parameters, and adsorption kinetics are some of the most well-known aspects of  $SO_4^{2-}$  adsorption performance. As a result, the adsorption capacity of electrocoagulation sludge for  $SO_4^{2-}$  removal from wastewater was investigated in this study. The experimental data for adsorbed  $SO_4^{2-}$  by electrocoagulation sludge was compared using the Langmuir and Freundlich isotherms. For the same system, two kinetic models, the pseudo-first order and the pseudo-second order, were explored. Adsorption isotherms are models that depict the distribution of adsorbate species between the liquid and adsorbent using linearly plotted graphs in accordance with a number of hypotheses regarding the heterogeneity or homogeneity of adsorbents, the type of coverage, and the potential interaction between the adsorbates (Langmuir and Freundlich models) [16,17]. As a result, the aim of this research was to recycle corrugated iron to create sludge that may be utilized as a raw material in a variety of wastewater purification applications. In our previously published work involving the electrocoagulation coagulation of sulphates, the parameters were optimized for the EC system to remove sulphates with an efficiency of 99.1% [18]. The fact that the corrugated iron is readily available, eco-friendly, it is reusable up to three cycles and does not require the use of chemicals, the produced sludge was applied in this manuscript as the adsorbent. The objective of this study was to determine effectiveness of EC sludge as an adsorbent in terms of removing the high concentration of  $SO_4^{2-}$  in wastewater. The study also establishes the ideal conditions for the removal of sulphate  $SO_4^{2-}$  utilizing the EC sludge produced by the usage of corrugated iron sheet.

## 2. Materials and Methods

### 2.1. Materials

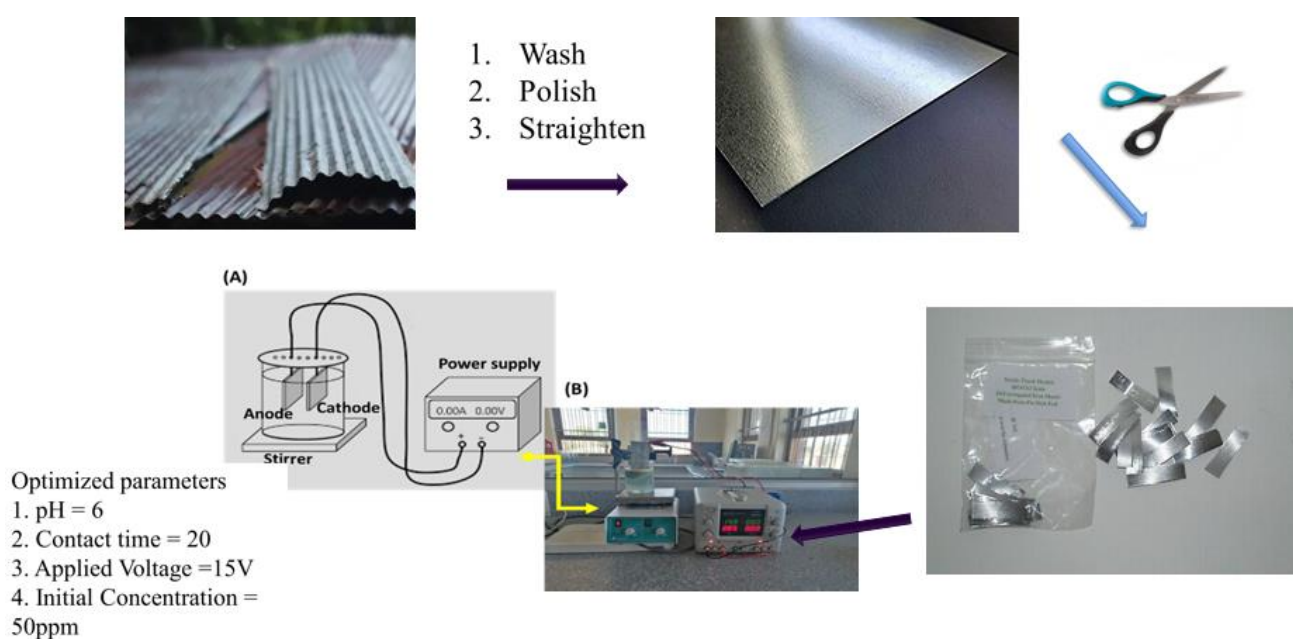
The wastewater from the battery plant was collected in South Africa's East London. Table 1 shows the composition of battery wastewater. Merck Company supplied the  $Na_2SO_4$ . Hydrochloric acid, HCl (37%), and sodium hydroxide, NaOH (96%), were acquired from Sigma-Aldrich (St. Louis, MO, USA), and all the solutions were made using ultrapure water.

**Table 1.** The composition of wastewater before and after the electrocoagulation process [18].

Parameters	Industrial Effluent (mg·L <sup>-1</sup> )	Removal by EC (%)	Synthetic Effluent (mg·L <sup>-1</sup> )	Removal by EC (%)	Discharge Limits (mg·L <sup>-1</sup> )
SO <sub>4</sub> <sup>2-</sup>	2678	99	3000	95	500
PO <sub>4</sub> <sup>3-</sup>	106	94	150	91	25
F <sup>-</sup>	60	94	100	90	5
COD	1459	90	1000	89	700
pH	4.39	-	2	-	6–11

### Continuous Electrocoagulation

The adsorbent sludge was generated through electrocoagulation studies using the previously published method [18]. The adsorption was performed using a corrugated iron electrodes under the optimal settings (pH 2, contact duration of 120 min, applied voltage of 15 V, and initial concentration of SO<sub>4</sub><sup>2-</sup> of 100 mg L<sup>-1</sup>, as shown in Scheme 1 [18].



**Scheme 1.** Preparation of the sludge (adsorbent) from (A) corrugated iron using (B) electrocoagulation system.

The electrocoagulation system was chosen because our previously published work in Yamba et al. reported that the electrical energy consumption increased linearly from 0.02588 to 0.1725 kWh/m<sup>3</sup> at 15 V, which is within the acceptable electrocoagulation range of 0.002 to 58 kWh/m<sup>3</sup>. This makes the operating costs of this technology of low cost effective. Furthermore, the cost of electrical energy usage might limit the use of EC in some circumstances. As a result, improving EC to treat a broader variety of pollutants using lower energy is desirable.

The wastewater from battery industry was collected from East London, in South Africa. The composition of battery wastewater, percentage removed by the electrocoagulation process and discharge limits are presented in Table 1 [18].

The sludge (adsorbent) obtained after electrocoagulation was then filtered and dried for roughly 8 h at 105 °C. The adsorbent was crushed and stored in a desiccator using a mortar and pestle. All the experimental results presented in this study employed the produced sludge as an adsorbent after the electrocoagulation process. According to the conventional approach, a spectrophotometer (HACH-DR 3900) was used to detect the amount of sulphate in the effluent.

## 2.2. Material Characterisation

A 500–4000 cm wavenumber infrared spectra of generated sludge was obtained using a Fourier-Transform Infrared spectrometer (Bruker-Alpha, Bremen, Germany) FTIR, model Nicolet 6700. X-ray diffraction (XRD, Ultima IV-Rigaku, Tokyo, Japan) advance, with Cu K $\alpha$ ,  $\lambda = 1.54 \text{ \AA}$ , scanning rate is  $1^\circ \text{ min}^{-1}$ , Germany) was used to validate the structure, composition, and phase identification of EC sludge. A scanning electron microscope (SEM), FE-SEM, Zeiss Crossbeam 540, Cambridge, UK, was used to obtain information about the surface topography and composition. The point of zero charge and the surface charge of the electrocoagulation sludge were identified using Zeta potential (Zetasizer Nano ZS-Malvern, Malvern, UK). Brunauer–Emmett–Teller (BET, Micromeritics TriStar II Plus, Leverkusen, Germany), was used to investigate the surface area and pore size measurements of the adsorbent.

## 2.3. Batch Adsorption Experiments

Batch adsorption studies were performed in a 600 mL Erlenmeyer flask filled with 500 mL of water containing the preferred  $\text{SO}_4^{2-}$  concentrations at various pH ranges of 2.0–10 for 120 min. Flasks containing varying concentrations of adsorbent were shaken in a shaker for 120 min. The effect of pH on  $\text{SO}_4^{2-}$  removal was investigated using adsorbent doses of 40 mg for  $\text{SO}_4^{2-}$  concentrations of 100 mg/L. The impact of the adsorbent dosage on percent removal was investigated using doses ranging from 20 to 200 mg/500 mL. The effect of  $\text{SO}_4^{2-}$  concentration on percent elimination was investigated using  $\text{SO}_4^{2-}$  concentrations ranging from 100 to 250 mg/50 mL at pH intervals of 2.0–10. The effect of contact time on percent elimination was evaluated from 20 to 120 min, whilst the other parameters remained unchanged. Adsorption isotherm tests were performed with varying  $\text{SO}_4^{2-}$  concentrations ranging from 100 to 250 mg/L while keeping the adsorbent dose constant at 40 g/500 mL. To ensure reproducibility and account for possible errors, control experiments were performed in triplicates. The studies were carried out at several pH levels (2.0, 4.0, 6.0, 8.0, and 10) and with different  $\text{SO}_4^{2-}$  concentrations (100, 150, 200, 250, and 300 mg/L) and dosages were 20, 40, 50, 100, 150, and 250 mg. The concentrations in solutions before and after adsorption were used to compute the quantity of  $\text{SO}_4^{2-}$  adsorbed.

The removal (%) of contaminant was calculated from Equation (1)

$$\% \text{ Removal} = \frac{C_0 - C_i}{C_0} \times 100\% \quad (1)$$

where  $C_i$  and  $C_0$  are the initial and final contaminants concentration in solution.

For energy consumption during electrocoagulation, the following equation was used.

$$\text{Energy consumption} = \left( \frac{\text{kwh}}{\text{m}^3} \right) \frac{\text{voltage} \times \text{current} \times \text{contact ime}}{\text{volume}} \quad (2)$$

In each experiment, the current was kept constant by controlling the voltage to monitor the energy consumption.

## 2.4. Adsorption Isotherms and Kinetic Studies

In order to characterize the link between the quantity of  $\text{SO}_4^{2-}$  adsorbed and its equilibrium concentration, both models were utilized in this investigation. The correlation coefficients were used to analyse the suitability of the isotherm circumstances. The Langmuir isotherm is important for monolayer adsorption on a surface with a limited number of identical sites. The model permits constant adsorption energies at the surface and prevents adsorbate immigration into the surface's plane [19].

The Langmuir equation is commonly expressed as:

$$C_e/q_e = \left( 1/q_m/K_1 \right) + \left( \frac{1}{q_m} \right) C_e \quad (3)$$

where  $C_e$  is the solution concentration at equilibrium ( $\text{mg L}^{-1}$ ),  $K_1$  is the affinity constant ( $\text{L}\cdot\text{mg}^{-1}$ ), and  $q_m$  is the maximum amount of adsorption ( $\text{mg g}^{-1}$ ). The slope and intercept of the linear plots of  $C_e/q_e$  vs.  $C_e$  were used to compute the maximum adsorption and Langmuir constant. This gave a straight line with a slope of  $1/q_m$ , which corresponds to full monolayer coverage ( $\text{mg g}^{-1}$ ), and an intercept of  $1/q_m K_1$ . The fundamental element of the Langmuir isotherm can be communicated by methods for dimensionless steady partition factor or balance boundary,  $R_1$ , which is calculated using the following equation:

$$R_1 = 1/(1 + K_1 C_0) \quad (4)$$

The kinetic research was carried out to remove  $\text{SO}_4^{2-}$  from wastewater. The pseudo first and pseudo second order models were proposed, and the equations are shown below:

Here, the first-order model is represented as Equation (5).

Where  $k_1$  = rate constant of pseudo-first-order model ( $\text{L min}^{-1}$ )

$$\ln(q_e - q_t) = \ln q_e - k_1 t \quad (5)$$

where  $k_1$  is the rate constant pseudo first order,  $q_e$  ( $\text{mg/g}$ ) is the amount of  $\text{SO}_4^{2-}$  adsorbed, and  $q_t$  ( $\text{mg/g}$ ) is the adsorbed  $\text{SO}_4^{2-}$  amount on the EC sludge at a specific given time ( $t$ ).

The linear equation for pseudo second order model is shown in Equation (6)

$$(t/q_t) = (1/k_2/q_e^2) + \left(\frac{1}{q_e}\right)t \quad (6)$$

where  $k_2$  ( $\text{g/mg/min}$ ) is the pseudo-second-order rate constant of adsorption, ( $q_e$ ) is the amount of sulphate adsorbed at equilibrium ( $\text{mg g}^{-1}$ ). Values of  $k_2$  and  $q_e$  were calculated from the intercept and the slope of the linear plots of  $t/q_t$  against  $t$ .

### 2.5. Preparation of Sludge (Adsorbent) for Reusability

The sludge that was used as an adsorbent in this work was obtained from our previously published work which involved the electrocoagulation experiments conducted with corrugated iron electrodes under optimized conditions; pH = 2, contact time = 120 min, applied voltage = 15 V and initial concentration  $\text{SO}_4^{2-} = 100 \text{ mg L}^{-1}$  as displayed in Schematic diagram 1 [18]. After each adsorption cycle, the adsorbent was washed with de-ionized water 5 times and re-dried in an oven set at  $80^\circ\text{C}$  for the adsorption of sulphate in the next cycle.

## 3. Results and Discussion

### 3.1. Characterization of Electrocoagulation Sludge

The sludge generated from the 600 mL of wastewater treated by the electrocoagulation process after 60 min of contact time was 2 g. The flocs of the sludge were compact, with dark and white crystals.

#### 3.1.1. FT-IR

Figure 2 shows the formation of iron oxide in the form of magnetite ( $\text{Fe}_3\text{O}_4$ ). As a result, the production of  $\text{Fe}_3\text{O}_4$  in electrochemical sludge magnetizes the products, which can be quite useful for catalytic activity and separation. However, FTIR spectrum also showed some peaks at  $1637 \text{ cm}^{-1}$  (C=O stretching band of carbonyl group),  $3438.66$  (stretching vibrations of CH,  $\text{CH}_2$  and  $\text{CH}_3$  groups,  $1065$  and  $868 \text{ cm}^{-1}$ , which were attributed to the stretching vibrations of CH,  $\text{CH}_2$  and  $\text{CH}_3$  groups),  $1637.63 \text{ cm}^{-1}$  (C=O stretching band of carbonyl groups) and  $1065.87 \text{ cm}^{-1}$  (the N-H bending from amide group). These analyses revealed the presence and interaction of several organic functional groups in the EC sludge, which are beneficial or aid in the adsorption process

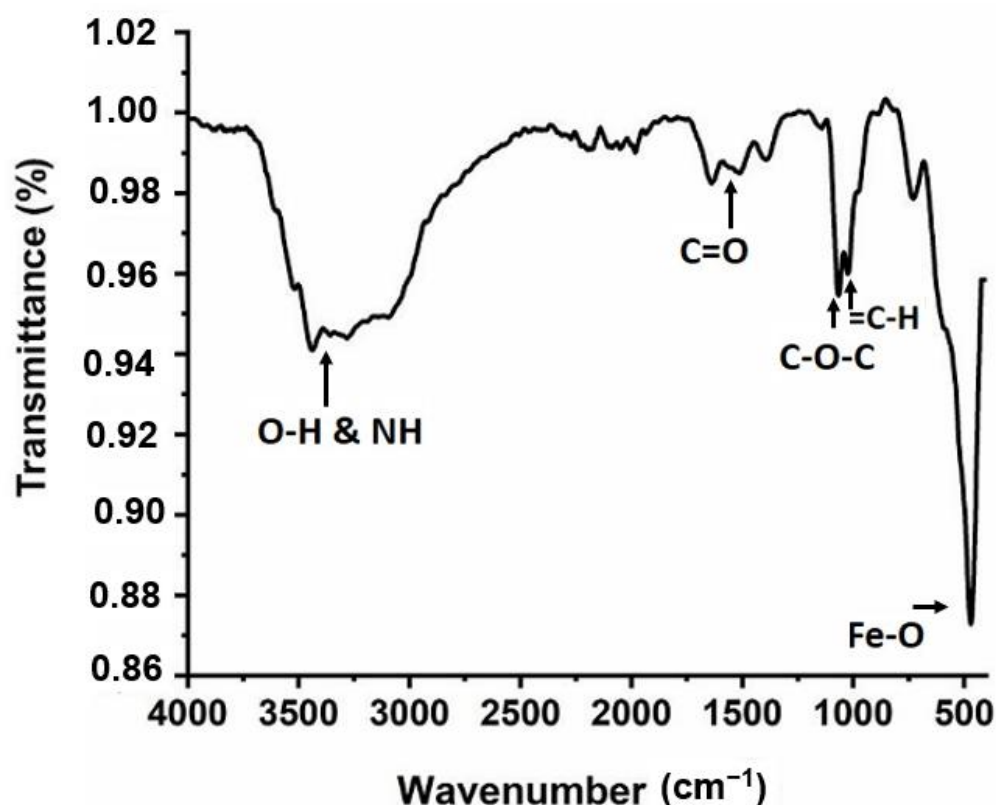


Figure 2. FT-IR spectrum of the sludge obtained after electrocoagulation.

### 3.1.2. XRD Patterns of Electrocoagulation Sludge

The EC sludge obtained by oxidation and coagulation is shown in Figure 3 after an XRD examination, which revealed that the sludge could be recycled to remove pollutants including  $\text{SO}_4^{2-}$ ,  $\text{PO}_4^{2-}$ ,  $\text{F}^-$ , and heavy metals in both artificial and actual wastewaters. A series of the characteristic peaks were observed in the XRD pattern at  $2\theta$  such as  $30.1^\circ$ ,  $38.9^\circ$ ,  $43.1^\circ$ ,  $54.5^\circ$ , and  $63.6^\circ$  corresponding to the diffractions of  $220^\circ$ ,  $311^\circ$ ,  $400^\circ$ ,  $422^\circ$ ,  $511^\circ$ , and  $440^\circ$  denoting the presence of iron oxide, which shows the crystalline nature of iron oxide [20].

Figure 3 also indicates the formation of Magnetite ( $\text{Fe}_3\text{O}_4$ ), with  $2\theta$  degrees of  $30.63^\circ$ ,  $35.97^\circ$ , and  $43.54^\circ$ , in the form of iron oxide.

Therefore, the existence of iron complexes and aluminium hydroxide complexes, which both contributed to the absorption of the  $\text{SO}_4^{2-}$ , is attributed to the peaks at  $2\theta = 48^\circ$  and  $68^\circ$ .

### 3.1.3. BET Surface Area Analysis

Table 2 shows that the surface area of the electrocoagulation sludge was  $231.247 \text{ m}^2/\text{g}$  with a total pore volume of 0.63. The porous material with diameters ranging from 19 nm to 43 nm seen from the nitrogen adsorption/desorption isotherm at 77 k was compared to a similar sludge data presented in the literature, including surface area analysis, as shown in Table 2. According to the International Union of Pure and Applied Chemistry's (IUPAC) classification, adsorbent pores are classified into three phases: microporous ( $<2 \text{ nm}$ ), mesopore (2–50 nm), and macropore ( $>50 \text{ nm}$ ). As a result, the obtained pore diameter follows the mesoporous and macropore classification. Similarly, the surface area is the most important factor that plays a significant impact in eliminating the necessary contaminants.

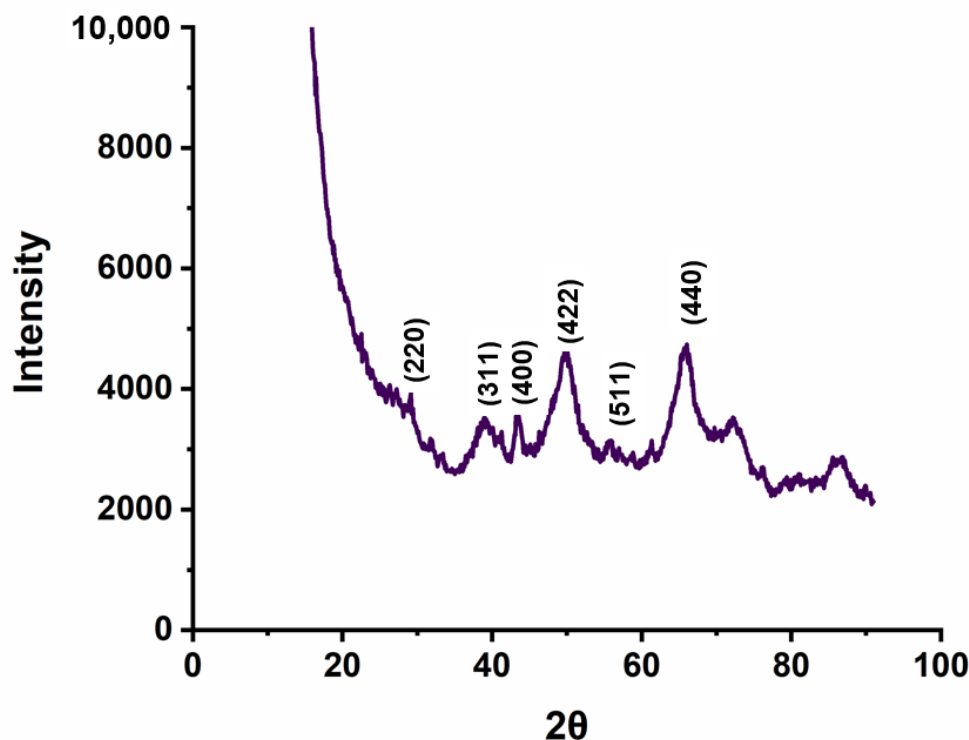


Figure 3. The XRD pattern of the EC sludge.

Table 2. Comparison of surface area and pore size analysis with literature Brunauer-Emmett-Teller (BET).

Material	Pore Volume (cm <sup>3</sup> /g)	Surface Area (m <sup>2</sup> /g)	Pore Diameter (nm)	Reference
Sludge	-	22.60 ± 0.20	10.70	[21]
Sludge	0.41	31.50 ± 0.03	23–52	[22]
Sludge	-	23–114	-	[23]
Dried activated sludge	-	183	-	[24]
Sewage sludge	-	67	30.0	[25]
Alum sludge	-	191	-	[26]
Paper mill sludge	-	-	-	[27]
EC sludge	0.63	231.247 ± 1.39	19–42	This study

#### 3.1.4. Textural Characterization by SEM

Figure 4 shows a SEM image of the EC sludge precipitates. The flocs of the sludge are compact, with dark and white crystals. These flocs agglomerate and suspended particles connect to the dark white floc through sweep floc coagulation. The particles generated sphere-like particles and oval particles created by the precipitation mechanism. Throughout the image, flake-shaped aggregates with a diameter of 2 μm were visible. Metal oxides such as iron oxide and aluminium oxide might be present in the homogeneous flake-shaped and spongy porous EC sludge [28].

Particles were found to be homogeneously scattered and almost spherical. In addition, a little white crystalline particle was discovered in the SEM micrograph, which agrees with the SEM results reported by Segura et al. [28].



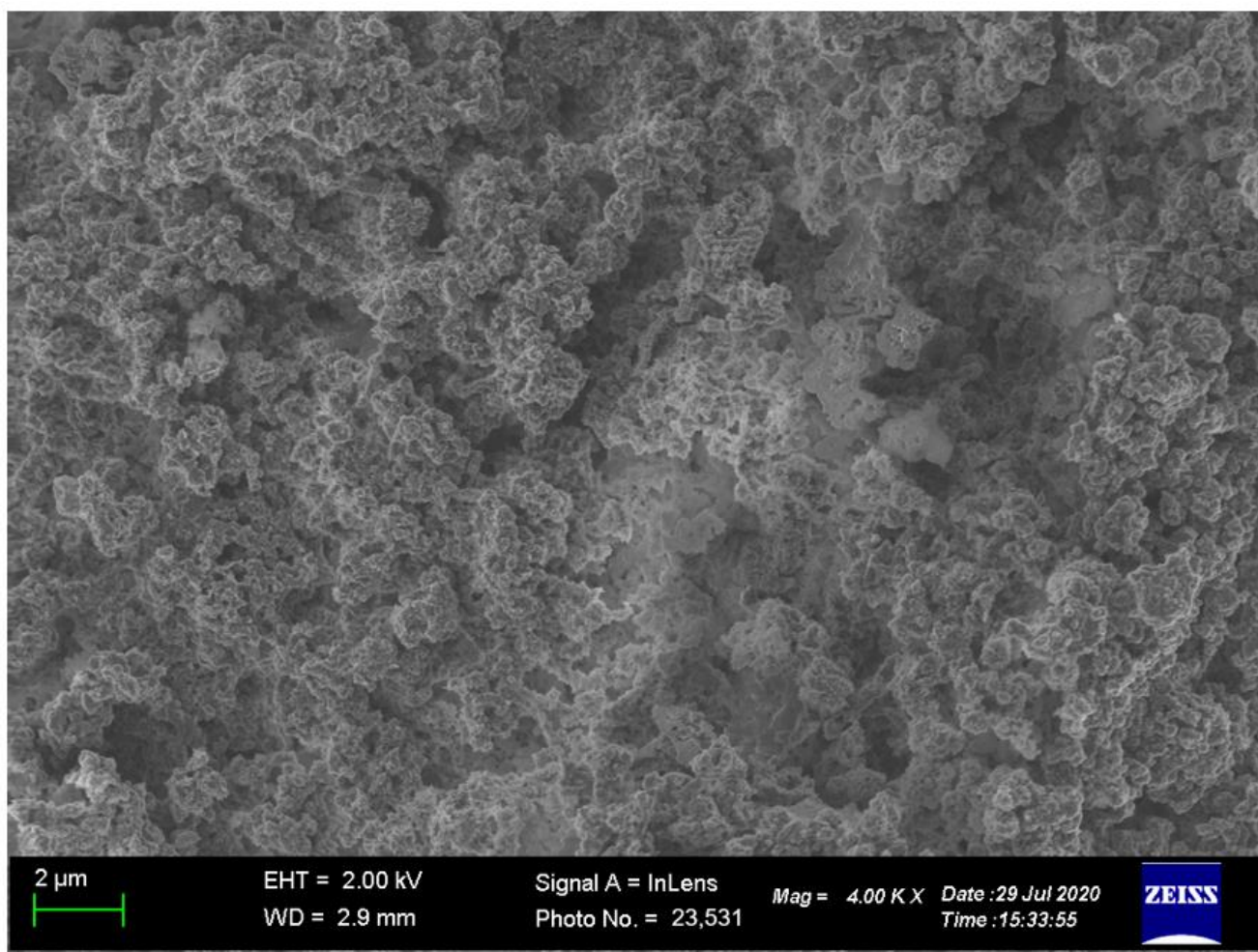


**Figure 4.** SEM image of EC sludge.

### 3.1.5. Zeta Potential of EC Sludge

The zeta potential was utilized to study the adsorbent's surface charge at various pH levels. As demonstrated in (Figure 5), the adsorbent is positively charged from pH 2 to pH 8, which might be due to the presence of amine groups in the sludge. The zero-charge point is seen at pH 9.6, implying that complexation of amine groups occurred below pH 9.6. Due to the adsorbent's high surface charge (51.9 mV) and the considerable electrostatic interaction between positively charged (adsorbent) and negatively charged (medium), a high removal efficiency of ( $\text{SO}_4^{2-}$ ) is predicted in acidic medium. Moreover, when the pH of the solution rises, the extremely low efficiency is anticipated. This can be characterized by the predicted significantly negatively charged surface of iron hydroxide, which is linked to the adsorption of iron hydroxoanions, which precludes sulphate adsorption.

### 3.2. Sulphate Removal by Electrocoagulation Sludge

The processes of sulphate ion removal from wastewater utilizing the electrocoagulation sludge as an adsorbent was examined by optimizing parameters such as starting pH solution, initial concentration, contact duration, adsorbent dosage, and adsorption isotherms to maximize its absorption and removal.

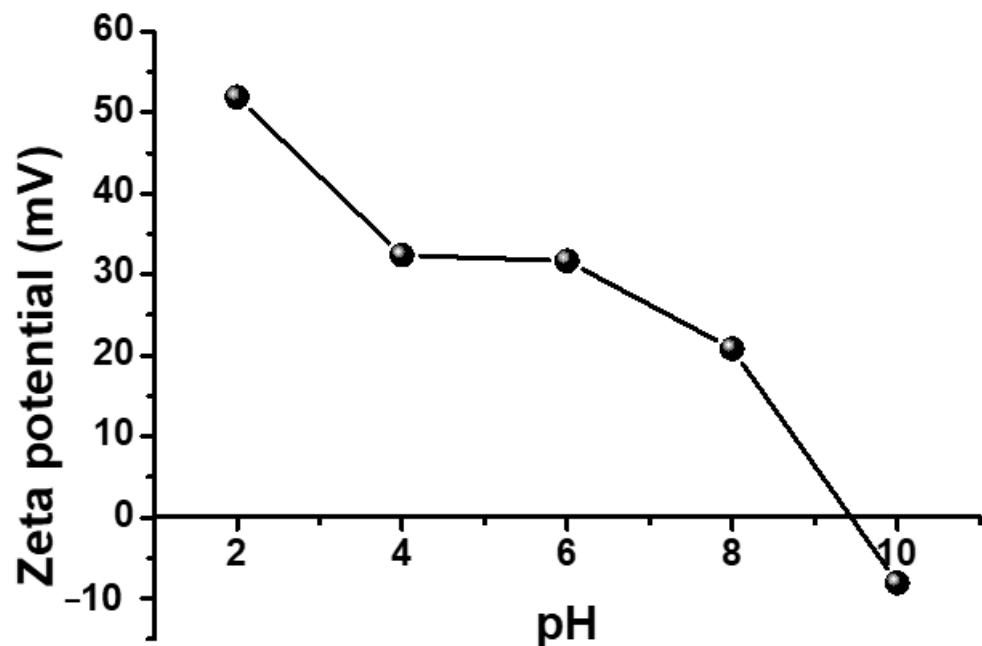


Figure 5. Zeta potential of EC sludge.

In the instance of  $\text{SO}_4^{2-}$  removal, pH values were varied from 2.0 to 12, as shown in Figure 6a, with pH 2.0 yielding the maximum sulphate removal percentage of 98.3 percent. Similarly, the proportion of substantial sulphate reduction increased from pH 4 to 6. At low pH, the adsorbent surface charge is comparatively linked with the hydronium ions ( $\text{H}_3\text{O}^+$ ) where the surface of the adsorbent becomes positively charged causing the electrostatic attraction between  $\text{SO}_4^{2-}$  ions to increase resulting in the production of more positively charged adsorption sites that necessitated a high sulphate removal percentage (Scheme 2). Moreover, as can be observed from Figure 6, more sulphate is chemisorbed at low pH due to the high charge neutralization. Above pH 8, bulkier species such as  $\text{Al}(\text{OH})_4^-$  are formed as the solution's pH rises. Hence, sulphate removal decreases as the pH of the solution increases. Additionally, the decarboxylation of the adsorbent surface charge and the presence of  $\text{OH}^-$ , which creates the electrostatic repulsion between the adsorbent and sulphate ions, provides the appearance that the adsorbent's surface charge is negative. Furthermore, Figure 6a shows that many pathways occurred since sulphate removal is pH dependent. Therefore, in all optimization experiments, the ideal pH of 2.0 was used.

According to Figure 6b, sulphate adsorption increases at low starting concentrations and declines as the solution concentration increases. The reason for this is that the surface charge of the adsorbents is more saturated by the sulphate ions at low starting concentrations. Furthermore, it is evident that the pH of the solution has an influence on the adsorption of sulphate ions.

Furthermore, Figure 7a illustrates how the contact time affects the percentage of sulphate removal. Since there were no available adsorption sites after the maximum percentage removal of sulphate, the percentage removal of sulphate increased with the period of contact time and reached equilibrium. High anode dissolution as the contact duration increased was also a contributing factor. The following Equation (7) can be used to calculate electrode dissolution in solution in accordance with Faraday's law [29,30],

$$C_{\text{electro}} = \text{MI}t / \text{ZFV} \quad (7)$$

where Z is the number of electrons transported, M is the molecular mass, F is the Faradays constant (96.485 C/mol),  $C_{\text{electro}}$  ( $\text{kg}/\text{m}^3$ ) is the theoretical quantity of ions created by current I (A) during a period of time t, and V is the volume ( $\text{m}^3$ ). After sufficient contact

time, a significant number of coagulants were formed, leading to a larger percentage of sulphate elimination after 120 min.

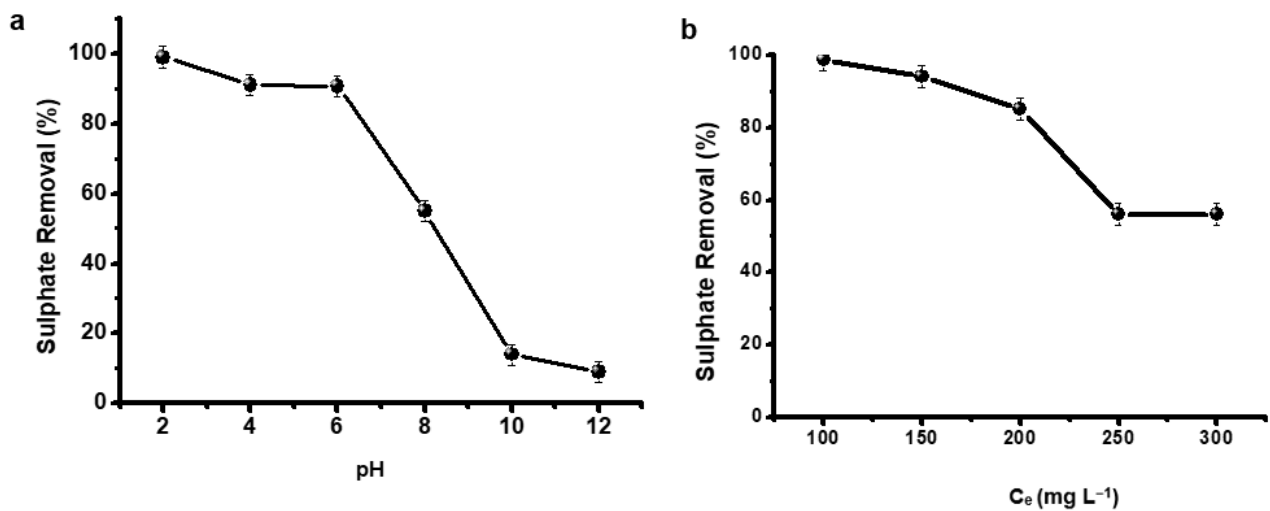
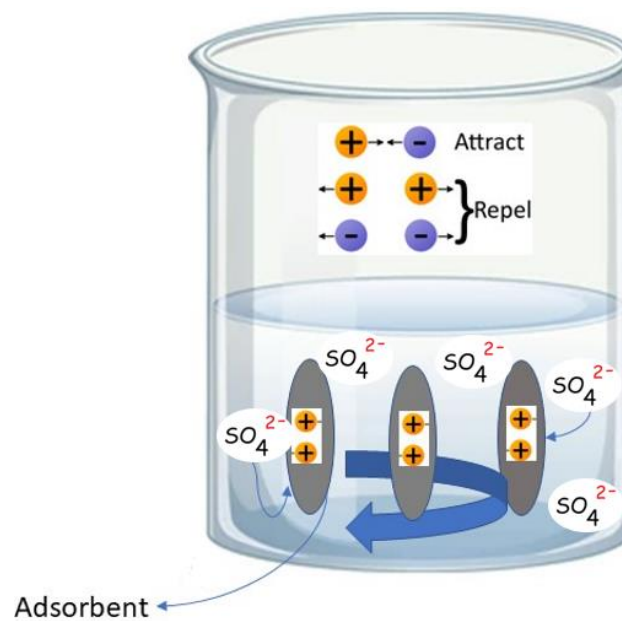


**Figure 6.** Effect of (a) pH and (b) initial concentration on the sulphate removal, conditions: contact time (120 min), dosage (40 mg), contact time (120 min), respectively.



**Scheme 2.** Adsorption of sulphates on iron and aluminium hydroxide cationic complexes.

The increase in adsorbent dose was shown to guide the growth in greater sulphate percentage removal in Figure 7b. The increase in positively charged surface area and sorption sites that results from raising the adsorbent dose may boost sulphate removal. The positively charged surface charge was exactly proportional to the mass of the adsorbent since the surface charge range was constant. Since 150 mg of adsorbent was used, the results shown in Figure 7b also showed that equilibrium adsorption of the sulphate removal had been achieved.

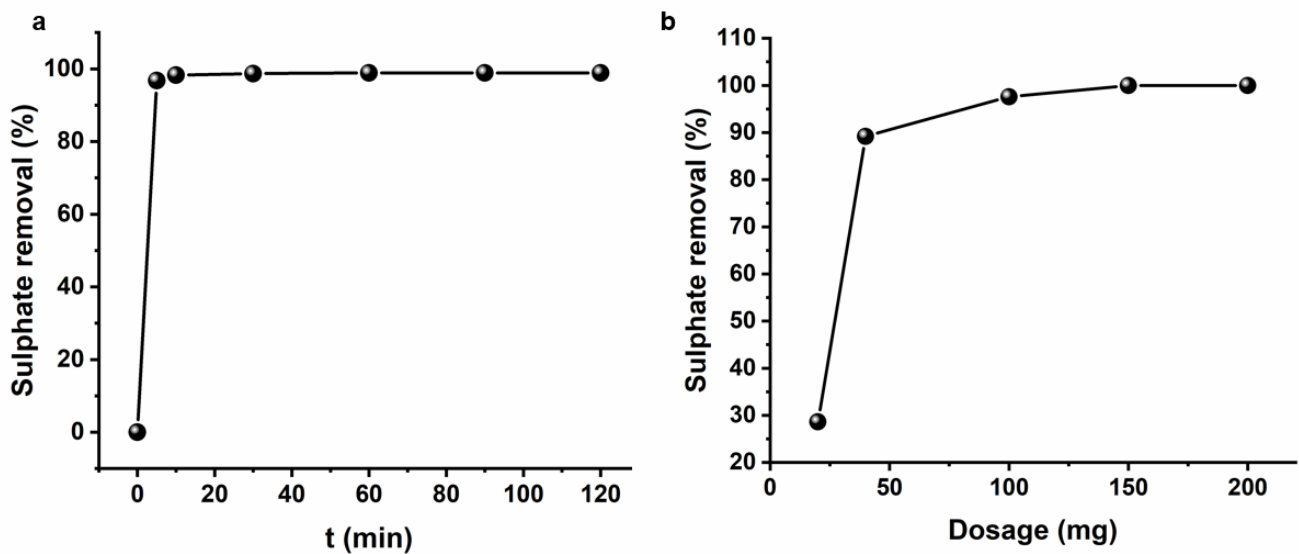


**Figure 7.** Effect of (a) contact time and (b) dosage on the sulphate removal, conditions: pH (2.0), initial concentration ( $100 \text{ mg L}^{-1}$ ) constant and pH (2.0), respectively.

### 3.2.1. Adsorption Isotherms

The adsorption of sulphates onto the EC sludge (adsorbent) was studied using adsorption isotherms. The adsorption of sulphates is mostly influenced by following optimised parameters pH 2, initial concentration  $100 \text{ mg/L}$ , dosage of  $150 \text{ mg}$  and contact time was  $120 \text{ min}$ . The experimental data was fitted to Langmuir isotherm (Equations (3) and (4)) and Freundlich isotherm according in Equation (9). The experimental data most likely fits well in Langmuir isotherm (Figure 8a), confirming the formation of a sulphate monolayer on the EC sludge as an adsorbent, which is expressed by Equation (3).

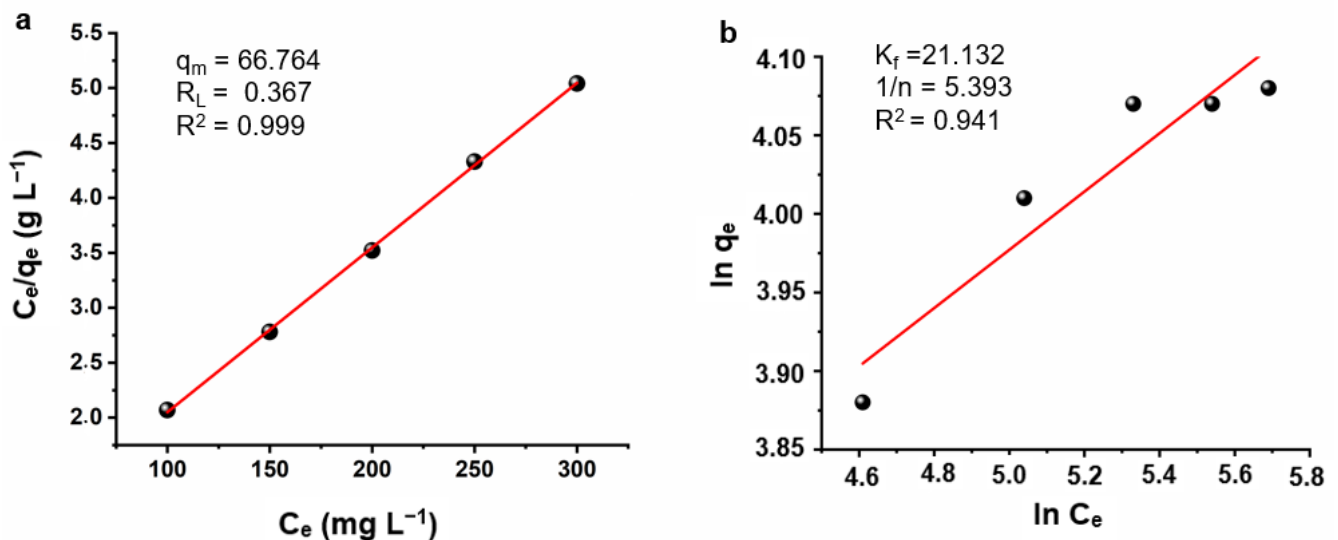


**Figure 8.** (a) Langmuir isotherm and (b) Freundlich isotherm for  $\text{SO}_4^{2-}$  removal.

Where  $C_e$  is the solution concentration at equilibrium ( $\text{mg L}^{-1}$ ),  $K_1$  is the affinity constant ( $\text{L} \cdot \text{mg}^{-1}$ ), and  $q_m$  is the maximum amount of adsorption ( $\text{mg g}^{-1}$ ). The slope and intercept of the linear plots of  $C_e/q_e$  vs.  $C_e$  were used to compute the maximum adsorption and Langmuir constant [21]. The  $R^2$  value illustrates that Langmuir model is better compared to the Freundlich model. The maximum amount of sulphate adsorbed ( $\text{mg g}^{-1}$ ) (adsorption capacity) on the EC sludge was  $66.76\%$  at an acidic pH, which is higher than the other materials reported in literature (Table 3). As explained in

Figure 1, in acidic pH, high concentrations of  $\text{Fe}^{2+}$ ,  $\text{Fe}^{3+}$  and  $\text{Al}^{3+}$  exists in the sludge to precipitate the sulphates. The increase in the adsorption capacity is enhanced by the existence of positive metallic hydroxide complexes that also co-precipitate sulphates in acidic pH. The dimensionless separation factor ( $R_L$ ) for Langmuir isotherm is calculated using Equation (4).

**Table 3.** Comparison of the maximum adsorption capacity of the adsorbent with other adsorbents.

Adsorbents	pH	$q_e$ (mg/g)	Contact Time (min)	Reference
Surfactant-modified palygorskite	4	3.24	4 h	[19]
Ba-modified blast furnace-slag geopolymer	7–8	119	1 h	[6]
Raw rice straw	2	11.68	2 h	[18]
Barium-modified acid-washed analcime	3–6	13.7	24 h	[22]
EC sludge	2	66.76	2 h	This study

Where  $R_L$  dimensionless steady partition factor or balance boundary,  $K_1$  is the affinity constant ( $\text{L}\cdot\text{mg}^{-1}$ ) and initial concentration of the analyte.  $R_L$  values show the nature of adsorption:  $R_L = 1$ , linear;  $R_L > 1$ , unfavourable;  $R_L = 0$ , irreversible; and  $0 < R_L < 1$ , favourable. The  $R_L$  values are found to be between 0 and 1. Therefore, it might be concluded that sulphate ions are effectively adsorbed onto the surface EC sludge.

Typically, the Freundlich isotherm model is used to describe the properties of a heterogeneous surface (Figure 8b). The linear version of the Freundlich isotherm is represented by Equation (8),

$$\ln q_e = (1/n \ln C_e) + (\ln K_f) \quad (8)$$

where  $K_f$  and  $1/n$  are the physical constants of the Freundlich adsorption isotherm, which are indicators of the adsorption capacity. When  $1/n$  is more than one, it indicates that the Freundlich mechanism was not favourable. Figure 8a,b displays a summary of the values for  $q_m$ ,  $K_1$ ,  $K_f$ ,  $R_L$ , and  $1/n$ .

### 3.2.2. Kinetic Study for $\text{SO}_4^{2-}$

The graph of  $\ln(q_e - qt)$  versus time (t) in Figure 9 yields a straight-line graph, which validates the use of the pseudo-first-order rate expression. The  $R^2$  value for sulphate adsorption is 0.370, confirming that the first order equation does not fit adequately over the full series of contact time and is typically used in the early stages of adsorption processes. As a result, the experimental data contradicts the pseudo-first-order kinetic.

The pseudo-second order model shown in Figure 9b obtained an  $R^2$  of 0.999, indicating that the data was well fit in this model. As a result, chemisorption influenced the surface adsorption rate, where physicochemical interactions between the two phases promoted sulphate removal from a solution [14].

### 3.3. Removal of $\text{SO}_4^{2-}$ and Other Pollutants from Real Industrial Wastewater

It is clear that the majority of typical industrial wastewater comprises more than one contaminant. In this study, a real wastewater sample was collected and analysed in one of the local battery industries. In addition, arsenic, chromium, and lead were discovered in real industrial effluent at varied concentrations, such as 98, 69, and 69, 78  $\text{mg}\cdot\text{L}^{-1}$ , respectively. The adsorbent removed more than 98.7% of the sulphate in the presence of As(III), Cr(VI), and Pb(II). Similarly, 95.6% arsenic, 92.3% chromium, and 91.6% lead were concurrently eliminated during the sulphate ion treatment. This could be due to the adsorbents' high surface area (231.4744  $\text{m}^2/\text{g}$ ), as proven by the BET analysis and Zeta

potential on the positive surface charge of the EC sludge [pH 2 (51.9 mV), pH 4 (32.4 mV), pH 6 (31.7 mV), and pH 8 (20.8 mV)].

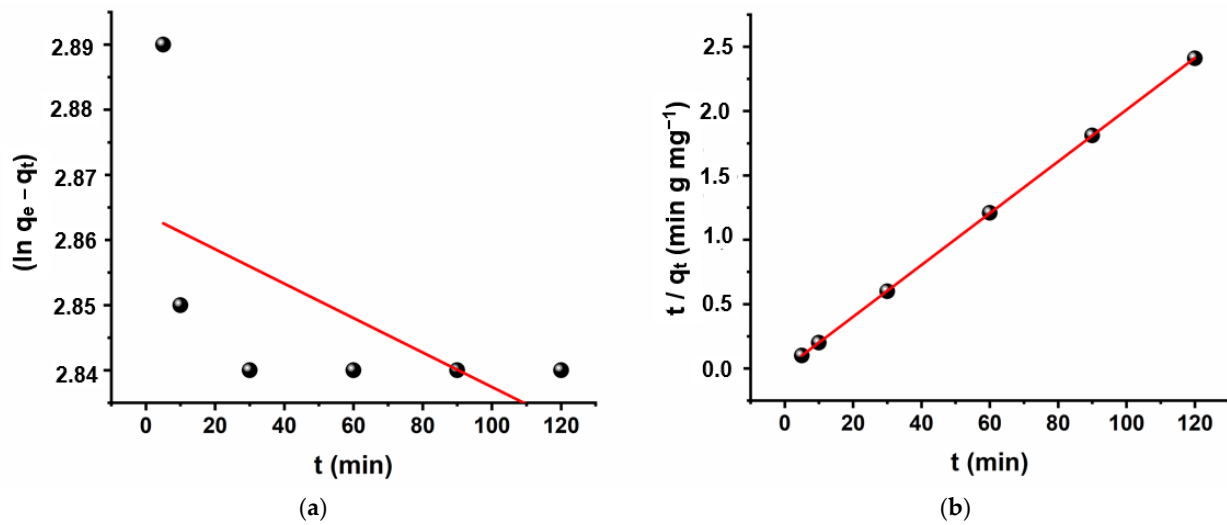


Figure 9. (a) pseudo-first-order model, (b) pseudo-second-order model.

### 3.4. Adsorbent Reusability/Recyclability

The reusability/recycling of the adsorbent is one of the most efficient techniques of minimizing treatment costs in any wastewater treatment. In this study, the adsorbent was utilized from cycle 1 to cycle 4, and after each cycle, it was cleaned with deionized water and dried at 80 °C for 4 h. Due to the high surface area that offers trapping of contaminants in wastewater, the results in Figure 10 demonstrate that the adsorbent was renewable and may be applied up to three cycles.

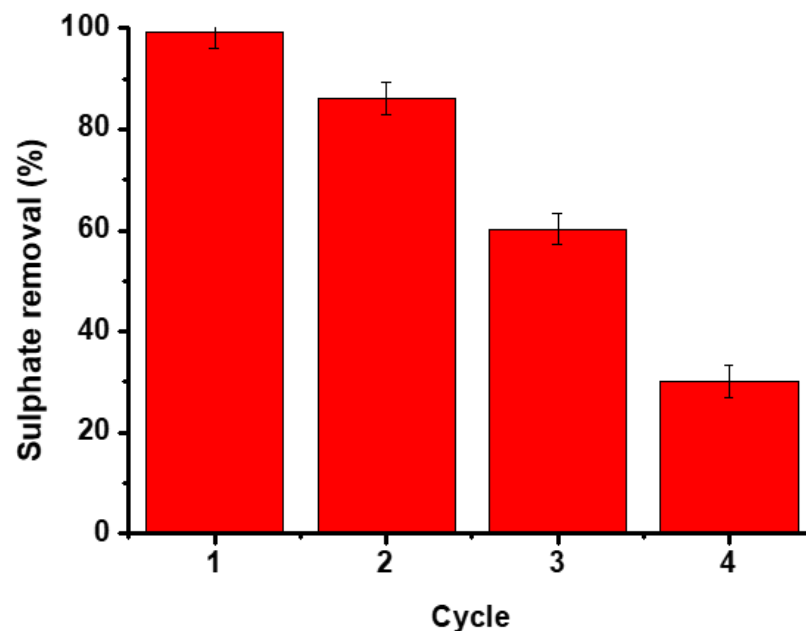


Figure 10. The use of an adsorbent to remove sulphate in various cycles.

Above pH 8, bulkier species like  $\text{Al}(\text{OH})_4^-$  were produced as the pH of the solution increased, hence a drastic decrease of sulphate removal was observed as the pH of the solution increased. Furthermore, surface charge of the adsorbent appeared to be negative due to the deprotonation of the adsorbent surface charge and the presence of  $\text{OH}^-$ , which caused the electrostatic repulsion between the adsorbent and sulphate ions.

#### 4. Conclusions

In this study, EC sludge that resulted from the electrocoagulation process was successfully applied in removing above 95% of sulphates in industrial effluents and synthetic samples at low pH. The iron, aluminium cationic hydroxide complexes were responsible for the adsorption of sulphates. The Langmuir equation was better fitted than the Freundlich isotherm. This confirmed the homogenous distribution of the active sites on the EC sludge. At different EC's sludges, the pseudo-second order kinetic model produced the best fitting experimental result which confirmed the removal of sulphate ions by chemisorption. The sludge can be recycled up 3 times to remove above 60% of sulphates. This work will assist in providing the analytical protocol to remove high concentrations of sulphates to prevent the secondary contamination and deterioration of the infrastructure of wastewater treatment plants in various municipalities.

**Author Contributions:** N.M.; conceptualization, resources, funding acquisition, supervision, writing—review and editing; S.Y.; methodology, software, validation; formal analysis, investigation, resources, data curation, writing—original draft preparation; N.C.H.-M.; supervision; writing—review and editing, T.L.Y.; project administration, R.M.; funding acquisition. All authors have read and agreed to the published version of the manuscript.

**Funding:** This work was funded by the Faculty of Science (URC/FRC) at the University of Johannesburg; National Research Foundation (CSUR), (SRUG200326510622), DST-Mintek NIC at the University of Johannesburg; the Centre for Nanomaterials Science Research, University of Johannesburg (UJ) South Africa and the Buffalo City Municipality, East London, Eastern Cape Province, South Africa.

**Institutional Review Board Statement:** Not applicable.

**Informed Consent Statement:** Not applicable.

**Data Availability Statement:** The data for this study is available on the following link Siyanda yamba project.

**Acknowledgments:** We would like to acknowledge the Department of Chemical Sciences at the University of Johannesburg for access to the instruments. Luthando Tshwenya and Simanye Sam are greatly acknowledged for their support during the project.

**Conflicts of Interest:** The authors declare no conflict of interest.

#### References

1. Godfrey, L.; Oelofse, S. Historical review of waste management and recycling in South Africa. *Resources* **2017**, *6*, 57. [[CrossRef](#)]
2. Baloy, O.; Sihaswana, D.; Maringa, M.; Sibande, J.; Oelofse, S.; Schubert, S. *National Waste Information Baseline Report*; Department of Environmental Affairs: Pretoria, South Africa, 2012.
3. Department of Environmental Affairs. *Status of Landfills in South Africa: Presentation to the Portfolio Committee*; Department of Environmental Affairs: Pretoria, South Africa, 2016.
4. Song, Q.; Li, J.; Zeng, X. Minimizing the increasing solid waste through zero waste strategy. *J. Clean. Prod.* **2015**, *104*, 199–210. [[CrossRef](#)]
5. Socio-Economic Rights Institute of South Africa (SERI). *Informal Settlements and Human Rights in South Africa: Submission to the United Nations Special Rapporteur on Adequate Housing as a Component of the Right to an Adequate Standard of Living*; Socio-Economic Rights Institute of South Africa (SERI): Johannesburg, South Africa, 2018; p. 26.
6. Attour, A.; Touati, M.; Tlili, M.; Amor, M.B.; Lapique, F.; Leclerc, J.P. Influence of operating parameters on phosphate removal from water by electrocoagulation using aluminum electrodes. *Sep. Purif. Technol.* **2014**, *123*, 124–129. [[CrossRef](#)]
7. Cao, W.; Dang, Z.; Zhou, X.Q.; Yi, X.Y.; Wu, P.X.; Zhu, N.W.; Lu, G.N. Removal of sulphate from aqueous solution using modified rice straw: Preparation, characterization and adsorption performance. *Carbohydr. Polym.* **2011**, *85*, 571–577. [[CrossRef](#)]
8. Dong, R.; Liu, Y.; Wang, X.; Huang, J. Adsorption of sulfate ions from aqueous solution by surfactant-modified palygorskite. *J. Chem. Eng. Data* **2011**, *56*, 3890–3896. [[CrossRef](#)]
9. Yilmaz, A.E.; Boncukcuoglu, R.; Kocakerim, M.; Karakas, I.H. Waste utilization: The removal of textile dye (Bomplex Red CR-L) from aqueous solution on sludge waste from electrocoagulation as adsorbent. *Desalination* **2011**, *277*, 156–163. [[CrossRef](#)]
10. Bener, S.; Bulca, Ö.; Palas, B.; Tekin, G.; Atalay, S.; Ersöz, G. Electrocoagulation process for the treatment of real textile wastewater: Effect of operative conditions on the organic carbon removal and kinetic study. *Process Saf. Environ. Prot.* **2019**, *129*, 47–54. [[CrossRef](#)]

11. Bayramoglu, M.; Kobya, M.; Can, O.T.; Sozbir, M. Operating cost analysis of electroagulation of textile dye wastewater. *Sep. Purif. Technol.* **2004**, *37*, 117–125. [[CrossRef](#)]
12. Jiménez, C.; Sáez, C.; Martínez, F.; Cañizares, P.; Rodrigo, M.A. Electrochemical dosing of iron and aluminum in continuous processes: A key step to explain electro-coagulation processes. *Sep. Purif. Technol.* **2012**, *98*, 102–108. [[CrossRef](#)]
13. Can, O.T.; Kobya, M.; Demirbas, E.; Bayramoglu, M. Treatment of the textile wastewater by combined electrocoagulation. *Chemosphere* **2006**, *62*, 181–187. [[CrossRef](#)]
14. Łuba, M.; Mikołajczyk, T.; Pierożyński, B.; Smoczyński, L.; Wojtacha, P.; Kuczyński, M. Electrochemical degradation of industrial dyes in wastewater through the dissolution of aluminum sacrificial anode of Cu/Al macro-corrosion galvanic cell. *Molecules* **2020**, *25*, 4108. [[CrossRef](#)] [[PubMed](#)]
15. Xiao, F.; Zhang, B.; Lee, C. Effects of low temperature on aluminum (III) hydrolysis: Theoretical and experimental studies. *J. Environ. Sci.* **2008**, *20*, 907–914. [[CrossRef](#)]
16. Ajenifuja, E.; Ajao, J.A.; Ajayi, E.O.B. Equilibrium adsorption isotherm studies of Cu (II) and Co (II) in high concentration aqueous solutions on Ag-TiO<sub>2</sub>-modified kaolinite ceramic adsorbents. *Appl. Water Sci.* **2017**, *7*, 2279–2286. [[CrossRef](#)]
17. Yan, L.G.; Yang, K.; Shan, R.R.; Yan, T.; Wei, J.; Yu, S.J.; Yu, H.Q.; Du, B. Kinetic, isotherm and thermodynamic investigations of phosphate adsorption onto core-shell Fe<sub>3</sub>O<sub>4</sub>@LDHs composites with easy magnetic separation assistance. *J. Colloid Interface Sci.* **2015**, *448*, 508–516. [[CrossRef](#)] [[PubMed](#)]
18. Yamba, S.; Moutloali, R.M.; Mabuba, N. Corrugated iron sheets for electrocoagulation of sulphate ions in industrial effluents. *Case Stud. Chem. Environ. Eng.* **2020**, *2*, 100061. [[CrossRef](#)]
19. Aljeboree, A.M.; Alshirifi, A.N.; Alkaim, A.F. Kinetics and equilibrium study for the adsorption of textile dyes on coconut shell activated carbon. *Arab. J. Chem.* **2017**, *10*, S3381–S3393. [[CrossRef](#)]
20. Subha, V.; Divya, K.; Gayathri, S.; Mohan, E.J. Applications of iron oxide nano composite in wastewater treatment–dye decolourisation and anti-microbial activity. *MOJ Drug Des. Dev. Ther.* **2018**, *2*, 178–184. [[CrossRef](#)]
21. Amanda, N.; Moersidik, S.S. Characterization of Sludge Generated from Acid Mine Drainage Treatment Plants. *J. Phys. Conf. Ser.* **2019**, *1351*, 012113. [[CrossRef](#)]
22. Munyengabe, A.; Zvinowanda, C.; Zvimba, J.N.; Ramontja, J. Characterization and reusability suggestions of the sludge generated from a synthetic acid mine drainage treatment using sodium ferrate (VI). *Heliyon* **2020**, *6*, e05244. [[CrossRef](#)]
23. Rakotonimaro, T.V.; Neculita, C.M.; Bussièrè, B.; Benzaazoua, M.; Zagury, G.J. Recovery and reuse of sludge from active and passive treatment of mine drainage-impacted waters: A review. *Environ. Sci. Pollut. Res.* **2017**, *24*, 73–91. [[CrossRef](#)]
24. Zare, H.; Heydarzade, H.; Rahimnejad, M.; Tardast, A.; Seyfi, M.; Peyghambarzadeh, S.M. Dried activated sludge as an appropriate biosorbent for removal of copper (II) ions. *Arab. J. Chem.* **2015**, *8*, 858–864. [[CrossRef](#)]
25. Nielsen, L.; Zhang, P.; Bandosz, T.J. Adsorption of carbamazepine on sludge/fish waste derived adsorbents: Effect of surface chemistry and texture. *Chem. Eng. J.* **2015**, *267*, 170–181. [[CrossRef](#)]
26. Mohammed, W.T.; Rashid, S.A. Phosphorus removal from wastewater using oven-dried alum sludge. *Int. J. Chem. Eng.* **2012**, *2012*, 125296. [[CrossRef](#)]
27. Kimura, K.; Wajima, T. Phosphate Removal Ability of Calcined Paper Sludge from Aqueous Solution—Effect of Calcination Temperature. *Int. J. Environ. Sci. Dev.* **2017**, *8*, 247–250. [[CrossRef](#)]
28. Bose, R.S.; Tiwari, M.K. Mine sludge waste recycling as bio-stimulant for applications in anaerobic wastewater treatment. *Water Sci. Technol.* **2019**, *79*, 425–434. [[CrossRef](#)] [[PubMed](#)]
29. Gutierrez-Segura, E.; Colin-Cruz, A.; Fall, C.; Solache-Rios, M.; Balderas-Hernández, P. Comparison of Cd-Pb adsorption on commercial activated carbon and carbonaceous material from pyrolysed sewage sludge in column system. *Environ. Technol.* **2009**, *30*, 455–461. [[CrossRef](#)] [[PubMed](#)]
30. Khandegar, V.; Saroha, A.K. Electrocoagulation for the treatment of textile industry effluent-A review. *J. Environ. Manage.* **2013**, *128*, 949–963. [[CrossRef](#)] [[PubMed](#)]